Conformation of a β-Adrenoceptor-Derived Signal Transducing Peptide As Inferred by Circular Dichroism and ^{1}H NMR Spectroscopy†

Hans Jung, Ralf Windhaber, Dieter Palm, and Klaus D. Schnackerz*

Theodor-Boveri-Institut für Biowissenschaften, Physiologische Chemie I, Universität Würzburg, Am Hubland, 97074 Würzburg, F.R.G.

Received October 30, 1995; Revised Manuscript Received March 19, 1996⊗

ABSTRACT: The peptide T345−359 representing the fourth intracellular loop of the avian β-adrenoceptor has been shown to strongly inhibit receptor-mediated adenylate cyclase activity [Münch, G., Dees, C., Hekman, M., & Palm, D. (1991) *Eur. J. Biochem. 198*, 357−364]. Circular dichroism and two-dimensional ^{1}H NMR techniques were used to investigate the three-dimensional structure of the peptide in trifluoroethanol, phospholipid micelles, and small unilamellar phospholipid vesicles. The prepared vesicles were tested for size distribution and stability by using electron microscopy, photon correlation spectroscopy, and ^{31}P NMR spectroscopy. The peptide T345−359 adopted a predominantly α-helical conformation in either trifluoroethanol or phospholipid micelles and vesicles. No structural differences were found for the conformation of the peptide in the presence of phospholipid micelles or vesicles, respectively, using 2D ^{1}H NMR techniques, suggesting a unique conformation of T345−359 when associated with model membranes. A computer-aided model of the micelle-associated peptide was derived. The relevance of the 3D structure of the intracellular loops of receptors to communicate with the G protein in the signal transduction cascade is discussed.

The β-adrenoceptor from turkey erythrocytes contains seven transmembrane helical segments, three intracellular loops, and a C-terminal cytoplasmic tail (Conklin & Bourne, 1993). Baldwin (1993) has recently proposed a model of G protein-coupled receptors which is based on the topological restraints of the loops, the proposed amphipathicity and residue variability of various helices, and the packing arrangement suggested by the low-resolution rhodopsin structure. The majority of primary sequence homologies reside within the hydrophobic transmembrane domains, whereas the hydrophilic loop regions are more divergent. The β-adrenoceptor activates the G_s[1] protein, which in turn stimulates or inhibits intracellular effectors or ion channels. Receptor chimeras, deletions, point mutations, and experiments with peptides that mimic receptor interactions with G protein have elucidated four regions of receptors thought to be involved in the specific G protein interaction. The proposed position of the transmembrane helices of the β-adrenoceptor is shown in Figure 1 (Yarden et al., 1986; O'Dowd et al., 1989). One way to obtain information about the interaction of the receptor and the G protein is to use synthetic peptides, representing the entire sequence of an intracellular loop or part of it, and incubate them under physiological conditions with native membranes containing the receptor, G protein, and an effector. Alternatively, as exemplified with peptides of the β-adrenoceptor, peptides might be incubated with G protein and adenylate cylase in the presence of model membranes to determine the production of cAMP (Palm et al., 1995). For the β-adrenoceptor from turkey erythrocyte membranes, peptide T284−295 (third loop) stimulates the production of cAMP, whereas

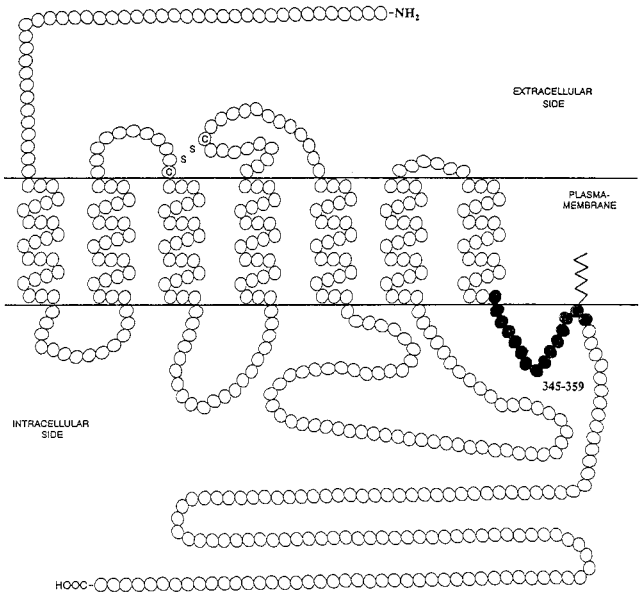

FIGURE 1: Topology of the transmembrane helices of the β-adrenoceptor from turkey erythrocytes. The model is adopted from Yarden et al. (1986) and O'Dowd et al. (1989). The position of the peptide T345−359 is indicated by the filled circles.

† The study was supported in part by grants Schn 139/11−3 and SFB 176, A10 of the Deutsche Forschungsgemeinschaft. H. Jung greatfully acknowledges the support by the "Graduiertenkolleg: NMR in-vivo und in-vitro für die biologische und medizinische Grundlagenforschung" of the Deutsche Forschungsgemeinschaft.

* Address correspondence to this author at Physiologische Chemie I, Biozentrum der Universität Würzburg, Am Hubland, 97074 Würzburg, Germany.

⊗ Abstract published in *Advance ACS Abstracts,* May 1, 1996.

[1] Abbreviations: CD, circular dichroism; COSY, correlated spectroscopy; 2D, 3D, two, three dimensional; DQ, double quantum; G protein, guanine nucleotide binding protein; G_S protein, stimulatory G protein; HPLC, high-performance liquid chromatography; NMR, nuclear magnetic resonance; NOE, nuclear Overhauser effect; NOESY, nuclear Overhauser enhancement spectroscopy; PC, phosphatidylcholine; PCS, photon correlation spectroscopy; ROESY, rotating frame Overhauser enhancement spectroscopy; TFE, trifluoroethanol; TOCSY, total correlation spectroscopy; TSP, 3-(trimethylsilyl)tetradeuteropropionate; TFA, trifluoroacetic acid.

S0006-2960(95)02575-X CCC: $12.00

peptides from other loops inhibit the adenylate cyclase system (Palm et al., 1990; Münch et al., 1991). The peptide T345−359 having the sequence RSPDFRKAFKRLLCF inhibits the hormone-stimulated adenylate cyclase to a residual 4% of its normal activity (Münch et al., 1991) and is therefore the most inhibitory peptide derived from intracellular loops of the β-adrenoceptor tested so far. It represents the fourth intracellular loop of the β-adrenoceptor (see Figure 1).

Inhibitory effects on the avian β-adrenoceptor adenylate cyclase complex have been reported for mastoparan, an amphiphilic tetradecapeptide from wasp venom (Münch et al., 1991). In contrast, mastoparan peptides directly activate members of the G_i and G_o protein family (Higashijima et al., 1990). In addition, two peptides, comprising the N- and C-terminal part of the third intracellular loop of the hamster β_2-adrenoceptor were found to stimulate the GTPase activity of the G_s protein, but not a preparation of G_i/G_o (Cheung et al., 1991). The presence of phospholipids was required in all cases, indicating the strong influence of the environment on the structure and function of peptides including mastoparans and their response to G proteins (Higashijima et al., 1988, 1990; Cheung et al., 1991). Structural studies on mastoparan in phospholipid bilayers have revealed an α-helix, positioned parallel to the plane of the membrane (Wakamatsu et al., 1992).

The β-adrenoceptor adenylate cyclase complex is one of the best-characterized hormonal signal transduction systems. Some information is known about the ligand-binding domain of biogenic amine or peptide receptors (Strader et al., 1994), but very little is known about the molecular basis of the activation of G proteins by receptors. The aim of this study is the elucidation of the 3D structure of peptide T345−359 in different solvents including phospholipid micelles and vesicles. The results of this study together with previous experiments on peptide T284−295 (third loop) of the β-adrenoceptor (Jung et al., 1995) and earlier investigations on mastoparan (Wakamatsu et al., 1992) provide a basis for correlating functional features with conformational properties of the intracellular peptide loops.

MATERIALS AND METHODS

Chemicals. Nucleosil columns were purchased from Macherey and Nagel. Protected amino acid derivatives were obtained from Calbiochem-Novabiochem. TFE, deuterated acetic acid, dimyristoyl-PC and lysomyristoyl-PC were products of Sigma. Deuterated dimyristoyl-PC and lysomyristoyl-PC were purchased from Avanti Polar Lipids, Alabaster, AL.

Peptide Synthesis and Purification. Peptides were synthesized as peptide amides using a Zinsser Analytic SMPS 350 A peptide synthesizer employing standard orthogonal F-moc chemistry. The peptide amides were obtained on Tentagel RAM resins (Rapp). A mixture of TFA/anisole/ethanedithiol was used for cleavage.

Preparation of Vesicles. Vesicles were prepared according to a procedure described by Higashijima et al. (1983) and Wakamatsu et al. (1983). Dimyristoyl-PC was dissolved in chloroform. A thin film of the phospholipid was produced in a glass tube by evaporating the solvent chloroform with gaseous nitrogen. Then the glass tube was kept *in vacuo* overnight to remove residual chloroform from the phospholipid film. The phospholipid layers were suspended in water or aqueous buffer solutions and sonicated for 20 min at 20 W. After sonication the solution was centrifuged for 10 min at 3000*g*. The supernatant contained the vesicles.

Photon Correlation Spectroscopy. PCS was carried out with a Autosizer 2c from Malvern.

Electron Microscopy. Vesicles were negatively stained with uranyl acetate and analyzed with a Zeiss EM10 transmission electron microscope (Gieffers & Krohne, 1991).

Circular Dichroism. CD spectra were recorded on a Jobin Ivon CD6 spectrometer. The measurements were carried out in cuvettes with 0.1 mm path length at peptide concentrations of 100 μM in water (pH 7.0). Spectra were recorded from 190 to 260 nm in 0.5 nm steps at a 1-s integration time at 23 °C. Ellipticity was recorded as mean residue molar ellipticity as calculated by the instrument software. After acquisition, spectra were smoothed by a polynomial fitting routine performed by spectrometer software. Quantification of the secondary structural components was done by comparison with computed spectra of model systems (Greenfield & Fassman, 1969).

NMR Spectroscopy. NMR samples contained 13 mM peptide, 5 mM deuterated acetate buffer, pH 4.15, 15% D_2O, and 60 mM deuterated lysomyristoyl-PC or 2 mM deuterated dimyristoyl-PC vesicles. ^{1}H NMR experiments were performed at 45 °C in 5-mm sample tubes on Bruker AM300SWB and AMX500WB spectrometers. The 2D experiments (Aue et al., 1976a; Bodenhausen et al., 1984) were performed in the phase-sensitive mode and quadrature detection in the F_1 dimension was achieved, analogous to the method of Redfield et al. (1975), using time-proportional phase increments (TPPI) (Marion & Wüthrich, 1983).

Typical acquisition parameters made use of a spectral width of 3000 or 5000 Hz, depending on the spectrometer used. Water suppression was achieved by a preparative presaturation pulse, usually 2.5 s long. In addition, the water resonance was saturated during mixing in NOESY and transfer NOESY experiments (Bell & Saunders, 1970; Jeener et al., 1979; Kumar et al., 1980; Wakamatsu et al., 1992). NOESY and transfer NOESY spectra were recorded with a mixing time of 250 ms, which was randomly varied over a range of ±10% to suppress zero-quantum cross peaks. In one-dimensional NOE experiments, the NOE increased linearly with irradiations up to 250 ms. DQ-COSY (Jeener, 1971; Bax & Freeman, 1981; Wider et al., 1984), ROESY (Bothner-By et al., 1984; Bax & Davis, 1985), *J*-resolved (Hahn, 1950; Aue et al., 1976b), and TOCSY (Braunschweiler & Ernst, 1983) experiments were performed according to standard pulse sequences. The length of the spin-lock pulse in ROESY experiments was 150 ms, with a B_1 field strength of 2.9 kHz corresponding to a 90° pulse of 85 μs. TOCSY spectra were obtained with the following pulse sequence: presaturation−90°−t_1−Sl_x−(MLEV-17)$_n$−Sl_x−acquisition. Before and after the MLEV-17 pulse train, a 2.5 ms trim pulse Sl_x was applied to defocus magnetization not parallel to the *x*-axis (Bax & Davis, 1985). The mixing pulse train was 55 or 33 ms for the 300 and 500 MHz instruments, respectively, including both trim pulses. The 90° pulse length for the mixing pulse train was 38 μs (B_1 = 6.6 kHz) for the AM300 and 21 μs (B_1 = 11.9 kHz) for the AMX500 spectrometer, respectively.

Depending on the spectral width, the number of t_1 increments in 2D experiments was usually adjusted to give a maximum t_1 time of 50 ms in the F_1 dimension. This

means about 300 t_1 values at a spectral width of 3000 Hz and 512 t_1 values at a spectral width of 5000 Hz. In the F_2 dimension, each free induction decay consisted of 1024 or 2048 data points, leading to an acquisition time of about 200 ms in F_2. *J*-resolved experiments were always performed with a time domain of 8192 data points in the F_2 dimension and 32 t_1 increments in the F_1 dimension. The sweep widths were 6400 Hz in the F_2 and 25 Hz in the F_1 dimension, and the size of the processed data file was 8192 times 256. One-dimensional experiments were typically performed with a 90° excitation pulse (10 or 6 μs at 300 or 500 MHz, respectively) and an acquisition time of 1.5 s. Fourier transformation of the acquired data was carried out on an Aspect 3000 computer using DISNMR software. The size of the processed data was 2048 points in both dimensions for phase-sensitive 2D experiments and 32768 points for 1D spectra. In the F_2 dimension, a Gaussian window function was applied, while in F_1 a sine-bell function, phase shifted by $\pi/3$, was used. Chemical shifts are expressed downfield of the methyl group of TSP.

Computational Procedures. The 3D structure of the peptide T345−359 in the presence of the micelles was modeled using 47 interresidue distance constraints and 12 dihedral angles Φ from NOESY and *J*-resolved NMR experiments. NOESY cross peaks were classified according to the number of levels in the contour plot. One level was assigned as weak, two levels as medium and three levels as strong, respectively. The intensity intervals were 2^n with n being the level number. Strong, medium, and weak cross peaks were interpreted as maximum interproton distances of 2.7, 3.8, and 5.0 Å, respectively. NN(i,i+1) cross peaks (two levels) were chosen as medium due to the known interproton distance of 2.8 Å for NN(i,i+1) in α-helical structures (Wüthrich, 1986). The dihedral angles Φ, describing the rotation around the axis of the distance Cα−N, were calculated from the measured coupling constants J(NH−Cα) using the equation of Karplus (1959). The parameters for the equation were taken from publications by Bystrow (1976) and Pardi et al. (1984). An error of 10% for the coupling constants of J(NH−Cα) resulted in a 7° error of the dihedral angle Φ. A first set of coordinate files for T345−359 was generated using the X-PLOR program, version 3.1 (Brünger, 1992), on a Silicon Graphics Iris Indigo computer. A family of six structures was obtained on the basis of the average energy value, fulfilling distance constraints with an error bound of 0.5 Å. The coordinate file with the lowest average energy value was used in further calculations applying the DISDM program on a VAX 11/730 computer. The resulting 3D structure was energy minimized by repetitive application of the refinement program EREF using the same computer.

RESULTS

Characterization of Model Membranes. The size distribution of the micelles and vesicles that were used as model membranes was determined with photon correlation spectroscopy. The size distribution of micelles derived from lysomyristoyl-PC gave 4 nm as the most frequent diameter of the micelles, consistent with values given by Vance and Vance (1985). When photon correlation spectroscopy was applied to vesicles derived from dimyristoyl-PC, diameters of about 20−35 nm were found to predominate (data not shown). The vesicles were large enough to be sized directly by electron microscopy. Electron microscopic images of vesicles obtained from dimyristoyl-PC (data not shown) revealed diameters that vary from about 20 to 40 nm, similar to the values obtained with photon correlation spectroscopy. The stability of vesicles was determined by observing the time course of the ^{31}P NMR signal in the presence of paramagnetic manganese ions (Hope et al., 1985). Upon addition of 5 mM $MnCl_2$, the NMR signal of dimyristoyl-PC decreased at once to 36% of the initial level. After 3 days the signal decreased by another 70%. This measurement indicates that after one day either 65% (assuming exponential signal decrease) or 75% (linear decay) of the vesicles were still intact. Therefore, the stability of the vesicles is sufficient to perform NMR experiments.

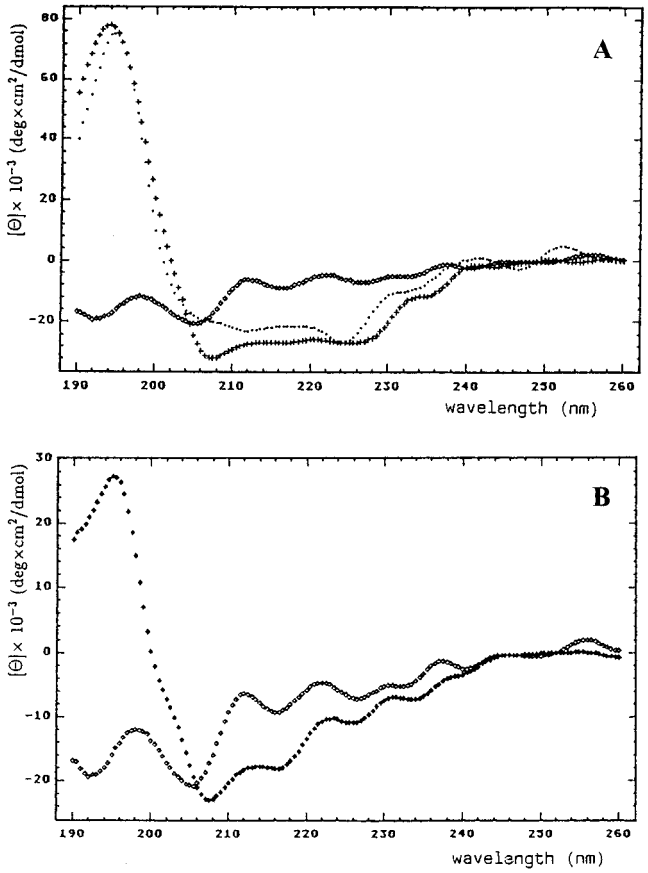

FIGURE 2: CD spectra of the peptide T345−359. (A) CD spectra of the peptide in the absence (open diamonds) and presence of 5 (dots) or 10 (crosses) mM micelles. The concentration of the peptide was 100 μM at pH 7.0 and 23 °C. (B) CD spectra of the peptide in the absence (open diamonds) and presence of 4 mM vesicles (crosses). Other conditions were the same as described for panel A.

CD Experiments. CD measurements of the peptide T345−359 were performed in different solvent systems. In pure water this peptide exhibits a random-coil (disordered) conformation with only about 20% α-helicity. CD spectra of the peptide dissolved in TFE/water mixtures at three different concentrations of TFE were measured (data not shown). The peptide T345−359 was found to be 80% α-helical in 50% TFE and 90% α-helical in 95% TFE. Similar values of α-helicity were determined upon addition of micelles derived from 5 and 10 mM lysomyristoyl-PC (Figure 2A). In the presence of vesicles derived from 4 mM dimyristoyl-PC, the CD results indicate that there was a conformational change from the disordered state in pure water to 60% α-helix (Figure 2B). It was not possible to

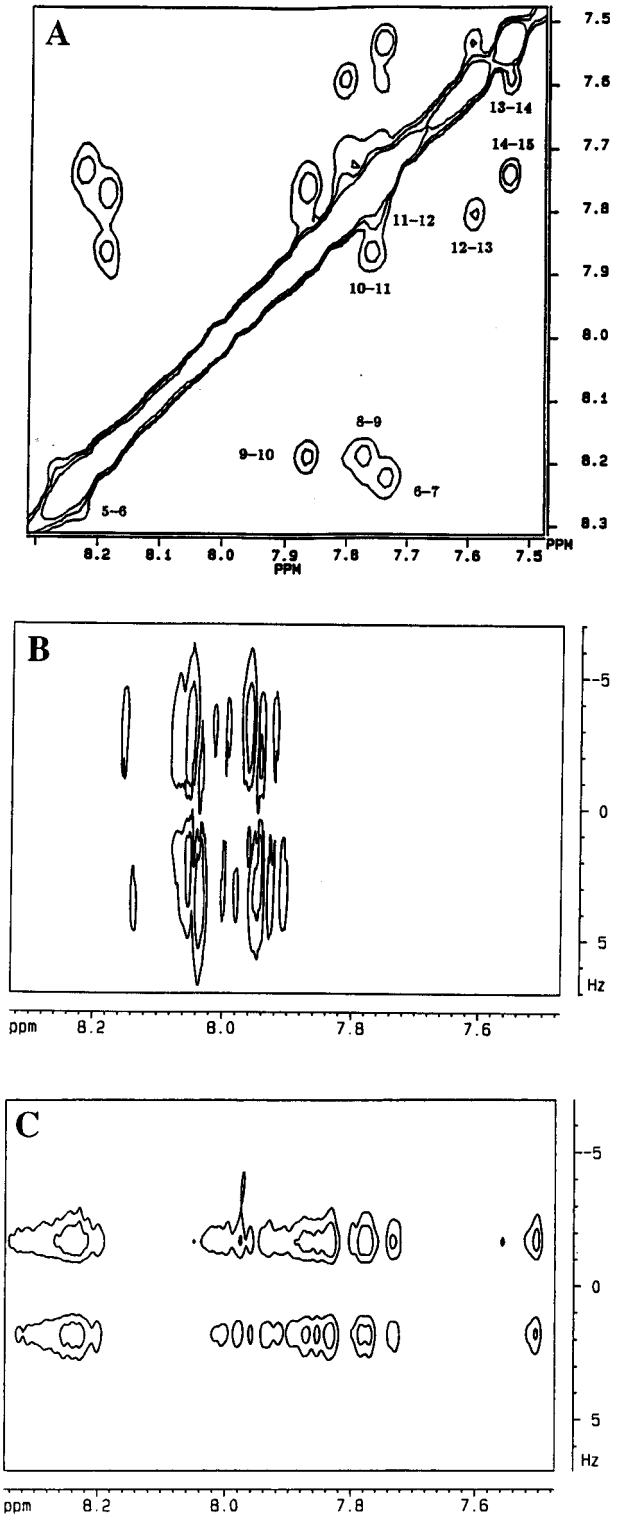

FIGURE 3: NH−NH region of the 500 MHz NOESY spectrum of the peptide T345−359 in the presence of micelles and NH regions of the 500 MHz *J*-resolved spectra. The peptide T345−359 (13 mM) was measured at pH 4.15 and 45 °C. (A) NH−NH region of the peptide T345−359 in the presence of 60 mM deuterated lyso-PC. The mixing time was 250 ms. The number located at the side of each cross peak labels the NH−NH correlation of the corresponding amino acid residue. (B) NH region of a 500 MHz *J*-resolved spectrum of the peptide T345−359 in aqueous solution. (C) NH region of a 500 MHz *J*-resolved spectrum of the peptide T345−359 in the presence of 60 mM deuterated lyso-PC.

work at higher concentrations of the dimyristoyl-PC vesicles because of light scattering effects which distorted the CD spectrum.

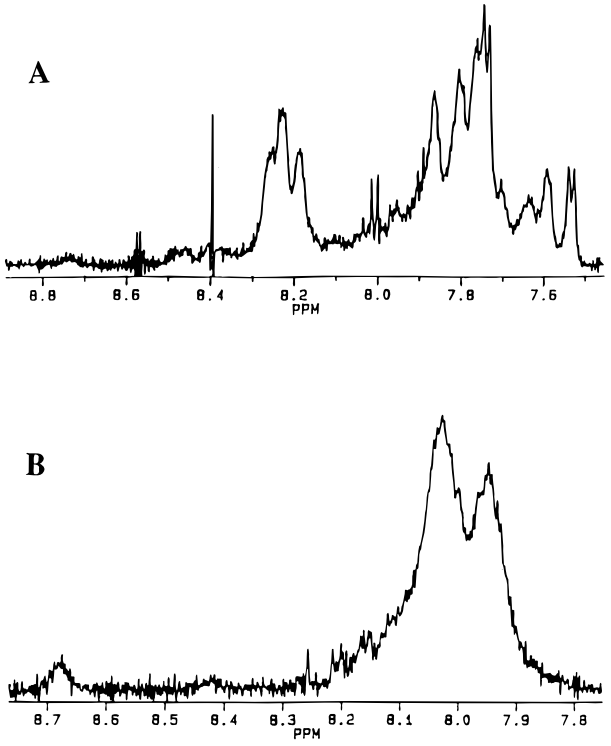

FIGURE 4: Backbone amide region of one-dimensional 500 MHz ^{1}H NMR spectra of the peptide T345−359 in the presence of micelles and vesicles. (A) The peptide T345−359 in the presence of 60 mM deuterated lyso-PC. (B) The peptide T345−359 in the presence of 2 mM dimyristoyl-PC. The conditions were the same as in Figure 3.

^{1}H NMR Experiments. The peptide T345−359 was studied by ^{1}H NMR techniques in aqueous solution and in the presence of 60 mM deuterated lysomyristoyl-PC micelles or 2 mM deuterated dimyristoyl-PC vesicles. In aqueous solution no secondary structural features of the peptide could be detected using NOESY and ROESY experiments. Only sequential connectivities were found. When the diagonal peaks were phased to be negative, the sequential cross peaks were positive, consistent with a small molecule with short correlation time ($\tau_c < 1$) (Wüthrich, 1986). *J*-resolved NMR experiments demonstrated that *J*(NH−Cα) was uniformly 6.0−6.4 Hz, providing further evidence for a random chain conformation (Figure 3B).

In the presence of micelles the peptide T345−359 adopted an α-helical conformation with the typical pattern of NN(*i*,*i*+1), αN(*i*,*i*+3), and αβ(*i*,*i*+3) cross peaks. The backbone amide region of a NOESY spectrum with NN(*i*,*i*+1) connectivities is shown in Figure 3A, while a one-dimensional portion of the spectrum is depicted in Figure 4A. All the detected cross peaks in the NOESY experiment are summarized in Figure 5A, and the assignment of the resonances is given in the Supporting Information. The signs of all cross peaks of the NOESY experiment are negative, suggesting that the small peptide binds to the large micelles. *J*-resolved NMR experiments provided coupling constants for *J*(NH−Cα) between 3.4 and 3.7 Hz in the presence of micelles (Figure 3C). The calculated dihedral angles Φ are in the range from −54° to −59°, typical for an α-helix (Φ = −57°) (Wüthrich, 1986).

Transfer NOE NMR experiments in the presence of vesicles yield lower sensitivity than found in the presence of micelles. Only few interresidue cross peaks were present,

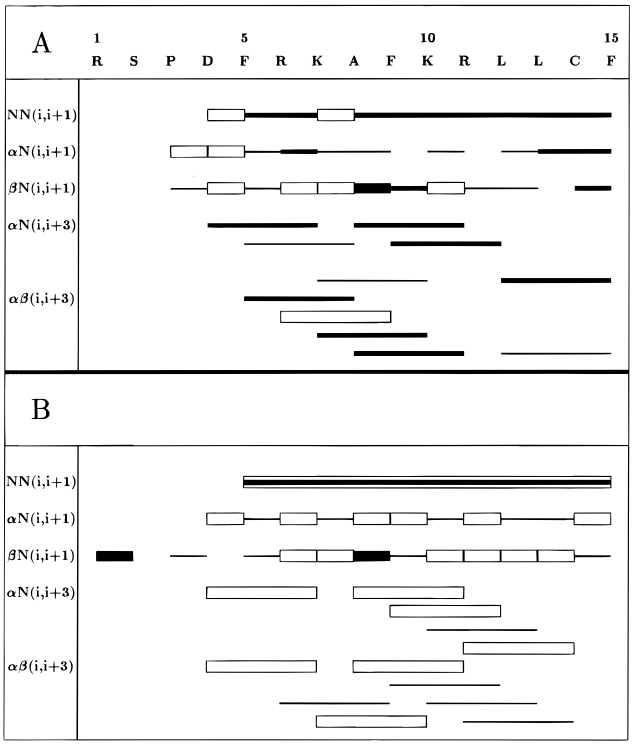

FIGURE 5: Summary of the observed cross peaks of the peptide T345−359 in the presence of micelles and vesicles. Thick, medium, and thin lines delineate the difference in strength of the detected connectivities. Medium size lines inside the open bars indicate that NN(i,i+1) cross peaks overlap and cannot be distinguished. Open bars indicate cross peaks that may be there but cannot be observed due to resonance overlap. (A) NOESY connectivities of T345−359 in the presence of 60 mM deuterated lyso-PC. (B) Transfer NOESY connectivities of the peptide T345−359 in the presence of 2 mM dimyristoyl-PC.

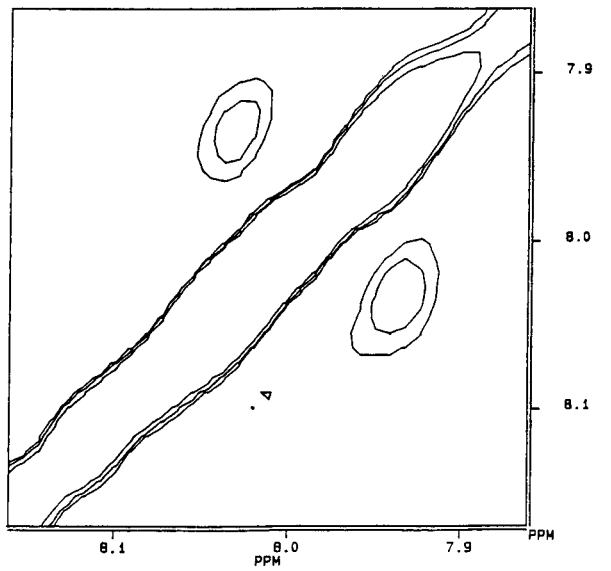

FIGURE 6: NH−NH region of a 500 MHz transfer NOESY spectrum of the peptide T345-359 in the presence of vesicles (2 mM dimyristoyl-PC). The conditions were the same as in Figure 3A.

but they were in agreement with the conformation detected in micelles. The transfer NOE makes use of the rapid exchange between the free and bound form of the peptide. The backbone amide region of the transfer NOESY spectrum with transfer NOE peaks is shown in Figure 6, while the one-dimensional spectrum of the backbone amide resonances

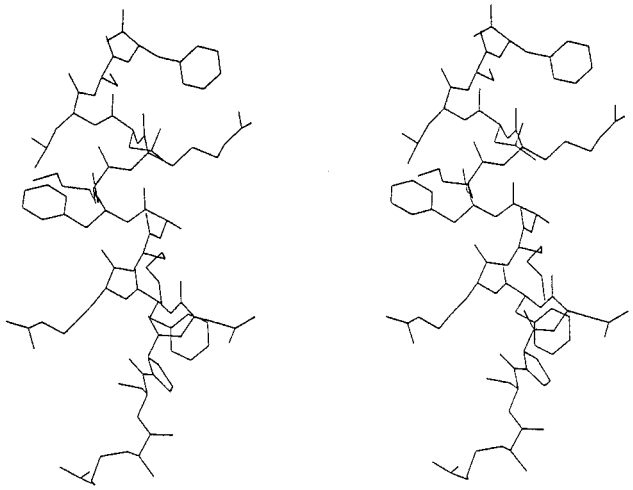

FIGURE 7: Stereoview of the 3D model of the peptide T345−359 in the presence of micelles.

is given in Figure 4B. The corresponding transfer NOESY connectivities are summarized in Figure 5B and the resonance assignment is given in the Supporting Information. The signs of the transfer NOESY cross peaks are negative, and the values for J(NH−Cα) are ranging between 3.0 and 3.1 Hz. These data coincide with results obtained in the presence of micelles within the limits of detection for J(NH−Cα) of $\pm$10%.

Computed 3D Structure. A stereoview of the 3D structure of the peptide T345−359 in the presence of lysomyristoyl-PC micelles is shown in Figure 7. The conformation was obtained by computer calculations using 47 interresidue distance constraints and 12 dihedral angles Φ from NOESY and J-resolved NMR data with subsequent energy minimization refinement. The 3D structure of the peptide T345−359, fulfilling all interresidue distance constraints and dihedral angles as determined by NMR within the error range, is an α-helix as found by circular dichroism. Only the two N-terminal residues remain flexible.

DISCUSSION

Much of the research on the interaction of receptors and G proteins has been focussed on the localization of contact sites, the sequences required for activation, and sequence elements involved in specificity (Kobilka, 1992; Ostrowski et al., 1992; Conklin & Bourne, 1993). In early studies, Dixon and co-workers (1987) showed that the removal of amino acid residues from either end of the third intracellular domain of the β-adrenoceptor uncoupled the receptor from G protein. In addition, mutations within the second intracellular domain and at the proximal end of the C-terminal tail, which proposedly might form a fourth intracellular loop, reduced the efficiency of the coupling (Kobilka et al., 1988; Strader et al., 1987). Several investigators including our own group have used synthetic peptides corresponding to sequences within various receptor domains to block or to stimulate the interaction of the receptor with the G protein (Palm et al., 1989, 1990, 1995; Münch et al., 1991; Higashijima et al., 1990; Cheung et al., 1991; Taylor et al., 1994). Considering the fact that this approach allows to assess the contribution of individual sites, it was found that at least two binding sites of the second, third, and fourth intracellular loops of G protein-coupled receptors are required

for functional and specific coupling. On the other hand, interaction of one G protein-docking site with some natural or synthetic G protein-activating peptide can already cause or modify G protein-dependent activation or inhibition, sometimes with preferential selectivity (Palm et al., 1995). One interesting group of peptides to which these qualifications apply are the mastoparans. These peptides directly activate members of the G_i protein family (Higashijima et al., 1990; Ross & Higashijima, 1994) but inhibit the hormone-stimulated activation of G_s protein (Münch et al., 1991). Biochemical and biophysical studies of these peptides have suggested that the cationic, amphiphilic α-helical nature of the mastoparans may be essential to their action (Sukumar & Higashijima, 1992). Recent data have suggested that the receptor exists in several dynamic states as reflected in changes in agonist affinity (Conklin & Bourne, 1993; Samana et al., 1993). Combining the results from other laboratories [reviewed in Strader et al. (1994)], a model emerges in which in the resting state of the receptor, the intracellular ends of the transmembrane domains, and the intracellular loops connecting them are in an inactive conformation. Upon agonist binding, a conformational change takes place in the receptor that opens the intracellular surface allowing the G protein to interact with the intracellular portion of the receptor. While the C-terminal portion of the third loop is important for G protein interaction, it may be more critical for maintaining the resting state of the receptor. It seems that one of the most promising avenues to correlate structure and function of the receptor−G protein interaction is to study peptides derived from intracellular loops of the receptor with regard to both aspects and compare them with mastoparan.

CD experiments in the presence of TFE revealed a high tendency of peptide T345−359 to adopt an α-helical conformation. Addition of micelles at concentrations above 5 mM phospholipids (50 times the concentration of the peptide) also resulted in the formation of an α-helix.

2D ^{1}H NMR data were used to determine the three-dimensional structure of the peptide T345−359. In the presence of micelles, 47 interresidue distance constraints and 12 dihedral angles were obtained. The resulting 3D structure is an almost complete α-helix where only residues 345 and 346 are flexible (Figure 7). It is conceivable that the flexibility of the N-terminal residues is necessary for the α-helix to align itself parallel to the plane of the membrane with its hydrophobic residues facing the lipid bilayer and its positive charges facing the the aqueous environment. Under those circumstances only one dynamic state would be possible, very similar to the situation found for mastoparan (Wakamatsu et al., 1992). It seems likely that loop 4 of the *β*-adrenoceptor has a similar α-helical conformation. The overall structure of the α-helix is amphiphilic, with five lysine and arginine residues located on one side and with hydrophobic side chains on the other side. The positive charges of the α-helix facing the hydrophilic intracellular side could represent a binding site of the receptor protein for the interaction with the G protein. In contrast, the peptide T284−295, located at the C-terminal end of the third loop of the *β*-adrenoceptor, is the only peptide derived from an intracellular loop of the *β*-adrenoceptor which stimulates the receptor-mediated adenylate cyclase (Münch et al., 1991). CD experiments of the peptide T284−295 similar to those described above showed 50% α-helix in the presence of micelles. Two-dimensional ^{1}H NMR studies on the peptide T284−295 disclose an α-helix only at its C-terminus, i.e., at residues 290−295, close to the transmembrane helix 6, but with a highly flexible region at the N-terminus (residues 284-289) (Jung et al., 1995). In accordance with the minor secondary structural constraints the same region in the native receptor protein might easily switch from an inactive to active conformation, thereby transmitting the positive signal provided by agonist binding to the receptor to the G protein. Since peptides derived from loop 2 are functionally inhibitory (Münch et al., 1991), it can easily be imagined that loops 2 and 4 of the *β*-adrenoceptor protein provide binding sites for the G protein, whereas loop 3 functions as the switch which can either be active or inactive.

A comparison of the peptide T345−359 and mastoparan brings about some interesting aspects. When mastoparan X is bound to a phospholipid bilayer, it forms an α-helix, positioned parallel to the plane of the membrane with its hydrophobic face within the bilayer and its four positive charges (three lysyl residues and the terminal amino group of isoleucine) facing toward the intracellular medium (Higashijima et al., 1983; Wakamatsu et al., 1992). Mapping of the G protein coupling domains using the site-specific peptides of the fourth loop of the *β*-adrenoceptor reveals that the overlapping peptides T338−352 and T345−359 are functionally very different. The former cannot compete with the complete signal tranduction system at all, whereas the latter inhibits the cascade to 4% of its basal activity (Münch et al., 1991). This comparison suggests that the C-terminal part of the peptide T345−359, i.e., KRLLCF, is mainly responsible for the inhibition. Interestingly, mastoparan X (INWKGIAAMAKKLL) has the closely related sequence KKLL at its C-terminus. In addition, the peptide T345−359 and mastoparan X are both almost totally α-helical with some flexibility at the N-terminal end. Comparison of the primary sequences of a large number of the α-subunits of G proteins (G_α) has shown that conserved sequences are found at the N-terminus, the C-terminus, and a region about 50 amino acids proximal to the C-terminus. These three regions of G_α are postulated to be the recognition sites for the receptor protein, as evidenced by mutations, specific antibody interactions, etc. (Conklin & Bourne, 1993). Cross linking of a particular mastoparan species to G_α followed by sequencing of a cyanogen bromide fragment revealed the N-terminus of G_α as the location of the cross link (Higashijima & Ross, 1991). On the assumption that the peptide T345−359 is bound to the same region of the G protein as mastoparan, it could be inferred that the peptide T345−359 interacts with the N-terminus of the G_α protein. However, more receptor-derived site-specific peptides have to be characterized structurally and functionally, to gain more accurate information about the coupling process.

ACKNOWLEDGMENT

We are indebted to Prof. Georg Krohne, Theodor-Boveri-Institut für Biowissenschaften, Lehrstuhl Zoologie I, Universität Würzburg, for the electron miscrocopy of the vesicles. We are likewise very grateful to Michael Käsbauer, Theodor-Boveri-Insitut für Biowissenschaften, Lehrstuhl Biotechnologie, Universität Würzburg, for the photon correlation spectroscopic measurements of the micelles and vesicles. Finally, we are very greatful to Drs. Paul F. Cook, Fort Worth, Texas, Bernd Hamprecht, Tübingen, and W. E.

Hull, Heidelberg, for critically reading the manuscript prior to publication.

SUPPORTING INFORMATION AVAILABLE

Two tables containing the assignment of the proton resonances of the peptide T345−359 in the presence of micelles and vesicles (2 pages). Ordering information is given on any current masthead page.

REFERENCES

Aue, W. P., Bartholdi, E., & Ernst, R. R. (1976a) *J. Chem. Phys. 64*, 2229−2246.

Aue, W. P., Karhan, J., & Ernst, R. R. (1976b) *J. Chem. Phys. 64*, 4226−4227.

Baldwin, J. M. (1993) *EMBO J. 12*, 1693−1703.

Bax, A., & Freeman, R. (1981) *J. Magn. Reson. 44*, 542−561.

Bax, A., & Davis, D. G. (1985a) *J. Magn. Reson. 63*, 207−213.

Bax, A., & Davis, D. G. (1985b) *J. Magn. Reson. 63*, 355−360.

Bell, R. A., & Saunders, J. K. (1970) *Can. J. Chem. 48*, 1114−1128.

Bodenhausen, G., Kogler, H., & Ernst, R. R. (1984) *J. Magn. Reson. 58*, 370−388.

Bothner-By, A. A., Stephens, R. L., Lee, J., Warren, C. D., & Jeanloz, R. W. (1984) *J. Am. Chem. Soc. 106*, 811−813.

Braunschweiler, L., & Ernst, R. R. (1983) *J. Magn. Reson. 53*, 521−528.

Brünger, A. T. (1992) X-PLOR Manual Version 3.1, Yale University, New Haven, CT.

Bystrow, V. F. (1976) *Prog. Nucl. Magn. Reson. Spectrosc. 10*, 41−82.

Cheung, A. H., Haung, R. R., Graziano, M. P., & Strader, C. D. (1991) *FEBS Lett. 279*, 277−280.

Conklin, B. R., & Bourne, H. R. (1993) *Cell 73*, 631−641.

Dixon, R. A. F., Sigal, I. S., Rands, E., Register, R. B., Candelore, M. R., Blake, A. D., & Strader, D. J. (1987) *Nature 326*, 73−77.

Gieffers, C., & Krohne, G. (1991) *Eur. J. Cell Biol. 55*, 191−199.

Greenfield, N., & Fasman, G. D. (1969) *Biochemistry 8*, 4108−4116.

Hahn, E. L. (1950) *Phys. Rev. 80*, 580.

Higashijima, T., & Ross, E. M. (1991) *J. Biol. Chem. 266*, 12655−12661.

Higashijima, T., Wakamatsu, K., Takemitsu, M., Fujino, M., Nakajima, T., & Miyazawa, T. (1983) *FEBS Lett. 152*, 227−230.

Higashijima, T., Uzu, S., Nakajima, T., & Ross, E. M. (1988) *J. Biol. Chem. 263*, 6491−6494.

Higashijima, T., Burnier, J., & Ross, E. M. (1990) *J. Biol. Chem. 265*, 14176−14186.

Hope, M. J., Bally, M. B., Webb, G., & Cullis, P. R. (1985) *Biochim. Biophys. Acta 812*, 55−65.

Jeener, J. (1971) Ampere International Summer School, Basko Polje, Yugoslavia.

Jeener, J., Meier, B. H., Bachmann, P., & Ernst, R. R. (1979) *J. Chem. Phys. 71*, 4546−4553.

Jung, H., Windhaber, R., Palm, D., & Schnackerz, K. D. (1995) *FEBS Lett. 358*, 133−136.

Karplus, M. (1959) *J. Phys. Chem. 30*, 11−15.

Kobilka, B. (1992) *Annu. Rev. Neurosci. 15*, 87−115.

Kobilka, B. K., Kobilka, T. S., Daniel, K., Reagan, J. W., Caron, M. G., & Lefkowitz, R. J. (1988) *Science 240*, 1310−1316.

Kumar, A., Ernst, R. R., & Wüthrich, K. (1980) *Biochem. Biophys. Res. Commun. 95*, 1−6.

Marion, D., & Wüthrich, K. (1983) *Biochem. Biophys. Res. Commun. 113*, 967−974.

Münch, G., Dees, C., Hekman, M., & Palm, D. (1991) *Eur. J. Biochem. 198*, 357−364.

O'Dowd, B. F., Hnatowicj, M., Caron, M. G., Lefkowitz, R. J., & Bouvier, M. (1989) *J. Biol. Chem. 263*, 15985−15992.

Ostrowski, J., Kjelsberg, M. A., Caron, M. G., & Lefkowitz, R. J. (1992) *Annu. Rev. Pharmacol. Toxicol. 32*, 167−183.

Palm, D., Münch, G., Dees, C., & Hekman, M. (1989) *FEBS Lett. 254*, 89−93.

Palm, D., Münch, G., Malek, D., Dees, C., & Hekman, M. (1990) *FEBS Lett. 262*, 294−298.

Palm, D., Münch, G., & Malek, D. (1995) *Methods Neurosci. 25*, 302−321.

Pardi, A., Billeter, M., & Wüthrich, K. (1984) *J. Mol. Biol. 180*, 741−751.

Redfield, A. G., Kunz, S. D., & Ralph, E. K. (1975) *J. Magn. Reson. 19*, 250−254.

Ross, E. M., & Higashijima, T. (1994) *Methods Enzymol. 237*, 26−37.

Samana, P., Cotecchia, S. Costa, T., & Lefkowitz, R. J. (1993) *J. Biol. Chem. 268*, 4625−4636.

Strader, C. D., Dixon, R. A. F., Cheung, A. H., Candelore, M. R., Blake, A. D., & Sigal, I. S. (1987) *J. Biol. Chem. 262*, 16439−16443.

Strader, C. D., Fong, T. M., Tota, M. R., Underwood, D., & Dixon, R. A. F. (1994) *Annu. Rev. Biochem. 63*, 101−132.

Sukumar, M., & Higashijima, T. 1992) *J. Biol. Chem. 267*, 21421−21424.

Taylor, J. M., Jacob-Mosier, G. G., Lawton, R. G., Remmers, A. E., & Neubig, R. R. (1994) *J. Biol. Chem. 269*, 27618−27624.

Vance, D. E., & Vance J. E. (1985) *Biochemistry of Lipids and Membranes*, Benjamin/Cummings Publishing Co., Menlo Park, CA.

Wakamatsu, K., Higashijima, T., Fujino, M., Nakajima, T., & Miyazawa, T. (1983) *FEBS Lett. 162*, 123−126.

Wakamatsu, K., Okada, A., Miyazawa, T., Ohya, M., & Higashijima, T. (1992) *Biochemistry 31*, 5654−5660.

Wider, G., Macura, S., Anil-Kumar, Ernst, R. R., & Wüthrich, K. (1984) *J. Magn. Reson. 56*, 207−234.

Wüthrich, K. (1986) *NMR of Proteins and Nucleic Acids*, Wiley, New York.

Yarden, Y., Rodrigues, H., Wong, S. K. F., Brandt, D. R., May, D. C., Burnier, J., Harkins, R. N., Chen, E. Y., Ramachandran, J., Ullrich, A., & Ross, E. (1986) *Proc. Natl. Acad. Sci. U.S.A. 83*, 6795−6799.

BI952575S